Effect of Graphitization on the Wettability and Electrical Conductivity of CVD-Carbon Nanotubes and Films

D. Mattia,[†] M. P. Rossi,[†] B. M. Kim,[‡] G. Korneva,[†] H. H. Bau,[‡] and Y. Gogotsi*,[†]

Materials Science and Engineering Department and A. J. Drexel Nanotechnology Institute, Drexel University, 3141 Chestnut Street, Philadelphia, Pennsylvania 19104, and Department of Mechanical Engineering and Applied Mechanics, University of Pennsylvania, 220 South 33rd Street, Philadelphia, Pennsylvania 19104

Received: February 22, 2006; In Final Form: March 24, 2006

The use of carbon nanomaterials in various applications requires precise control of their surface and bulk properties. In this paper, we present a strategy for modifying the surface chemistry, wettability, and electrical conductivity of carbon tubes and films through annealing in a vacuum. Experiments were conducted with 60−300 nm nanotubes (nanopipes), produced by noncatalytic chemical vapor deposition (CVD) in a porous alumina template, and with thin films deposited by the same technique on a glassy carbon substrate having the same structure and chemistry of the CNTs. The surface of the as-produced CVD-carbon, treated with sodium hydroxide to remove the alumina template, is hydrophilic, and the bulk electrical conductivity is lower by a factor of 20 than that of fully graphitic multiwalled nanotubes (MWNT) or bulk graphite. The bulk electrical conductivity increases to the conductivity of graphite after annealing at 2000 °C in a high vacuum. The analysis of CNTs by transmission electron microscopy (TEM) and Raman spectroscopy shows the ordering of carbon accompanied by an exponential increase of the in-plane crystallite size, L_a, with increasing annealing temperature. Environmental scanning electron microscopy (ESEM) was used to study the interaction of CNT with water, and contact angle measurements performed using the sessile drop method on CVD-carbon films demonstrate that the contact angle increases nearly linearly with increasing annealing temperature.

Introduction

Nanostructured carbon materials are considered for various applications in nanotechnology ranging from factory-on-a-chip to chemical sensors. Carbon nanotubes, in particular, are potential building blocks for nanofluidic devices,[1−3] where control of wetting[4] and transport properties[5] at the nanoscale is required.

It has been previously shown that as-produced CVD-carbon nanotubes can readily imbibe water and other polar liquids[6] and that preferential condensation occurs in these tubes inside the chamber of an ESEM.[1] These results appeared to contradict the common knowledge that graphite is not wet by water.[7,8] This apparent contradiction was solved by elucidating the effect of surface terminations of CVD-carbon, especially caused by treatment with NaOH, necessary to dissolve the alumina template, which strongly alters the wetting behavior of both carbon nanotubes and films, with the contact angle decreasing from 79° prior to treatment to 44° after it.[4]

Another key property of interest is the electrical conductivity. It is known that the electrical conductivity of graphitic carbon varies from 100 to 5000 S/m for low-temperature CVD grown disordered carbon containing hydrogen and various functional groups[9−11] to 20 000 S/m for partially ordered PECVD-carbon,[12] to $(2-4) \times 10^5$ S/m for well-ordered graphite (in plane conductivity).[10] No systematic study of the effect of the annealing temperature on the electrical conductivity of template based CVD-carbon nanotubes is available.

One simple way to modify and control the chemistry and structure of nanostructured carbon materials is through a graphitization process, with progressive removal of the surface terminations and increasing L_a. High-temperature annealing of MWNTs is generally used to heal defects in the graphitic walls resulting from the synthesis process as well as to eliminate the metal catalyst used to produce the tubes.[13] When carbon nanotubes are used as cellular probes, the choice of softer or stiffer graphitic tubes can be important for penetrating the cell membrane and controlling tube deflection inside the cell.[14]

Graphitization of turbostratic carbon leads to its transformation to well-ordered graphite. CNTs produced by pyrolysis of propylene showed a significant increase in the degree of ordering of the (002) planes after heating to 2800 °C under Ar flow.[15] Transmission electron microscope (TEM) micrographs of nanotubes annealed at 2400 °C showed a well-ordered graphite wall structure.[16] Low-temperature graphitization (545 °C) of template CNTs in the presence of a nickel catalyst has also been reported.[17] However, little is known about the effect of annealing on the properties of carbon nanotubes. In this paper, we report on the effect of the annealing temperature on wetting and the electrical conductivity of CVD-carbon nanotubes and films.

Materials and Methods

Carbon nanotubes were produced by noncatalytic CVD using porous alumina membranes as templates.[18,19] A commercial alumina membrane (Whatman Anodisc, nominal pore diameter: 200 nm ± 10%; 60 μm thickness) was used to produce nanotubes with external diameters up to 300 nm. Nanotubes with a nominal external diameter of about 60 nm and length up to 90 μm were synthesized using an in-house produced alumina

* Corresponding author. Tel.: (215) 895-6446. Fax: (215) 895-1934. E-mail: gogotsi@drexel.edu.
[†] Drexel University.
[‡] University of Pennsylvania.

10.1021/jp061138s CCC: $33.50
Published on Web 05/03/2006

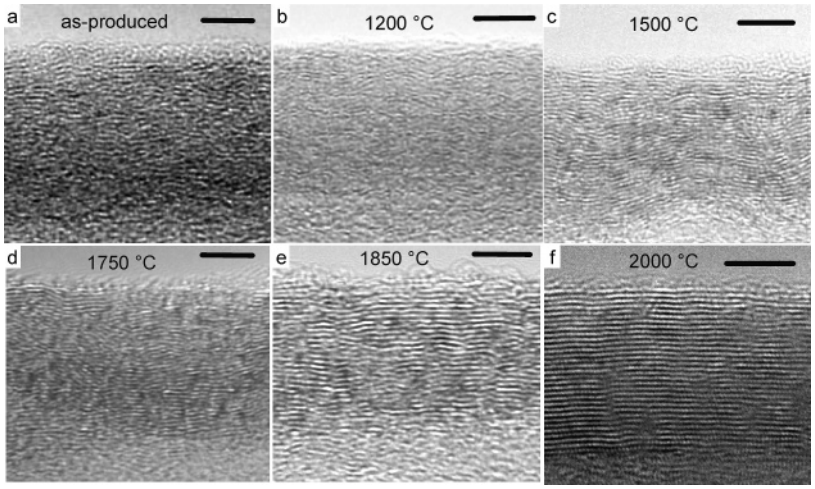

Figure 1. TEM micrographs of the walls of (a) as-produced nanotubes and those annealed at (b) 1200 °C, (c) 1500 °C, (d) 1750 °C, (e) 1850 °C, and (f) 2000 °C. The initial, disordered carbon structure is converted into a more and more perfect graphitic structure with an increasing annealing temperature. Scale bar is 5 nm.

membrane with smaller pores. This membrane was produced using a modified version of methods described in the literature:[20−24] a 20 × 40 × 0.01 mm^3 piece of aluminum foil, 99.99% purity from Alfa Aesar, was degreased in dichloromethane for 5 min. Subsequently, the aluminum was electropolished in 20% v/v perchloric acid in ethanol for 5 min at a constant voltage of 20 V (DC) in an acetone-dry ice bath (approximately −77 °C) using a stainless steel plate as a cathode. After electropolishing, the Al was rinsed in ethanol and then in deionized water (17.8 MΩ). The resulting mirrorlike electropolished aluminum was anodized in 0.3 M oxalic acid at a constant voltage of 60 V (DC) for 10−12 h at 10 °C. After anodization, the membrane was rinsed with deionized water, dried, and the anodized side of the aluminum foil was covered with nail polish to protect pores during the post-treatment process. After removal of the remaining aluminum in cupric solution,[25] the porous layer became transparent. To open the barrier layer, the anodized alumina was dipped in 0.1 M phosphoric acid for 1 h at room temperature. Finally, the membrane was rinsed accurately in acetone to remove the nail polish.

To release the nanotubes from the template, alumina was dissolved in a boiling 1 M solution of NaOH. The resulting, free-standing nanotubes were perfectly straight, open-ended, and had a typical wall thickness of 15−20 nm (Figure 1a).[1,4]

Polished (4000 SiC paper) and degreased glassy carbon tokens (GL-200 from Toyo Tanso Co.) were used as a substrate for CVD-carbon film deposition. The resulting thin films had the same chemistry and structure as the CVD nanotubes.[4]

Deionized water (surface tension 72 mN/m) and a nonpolar fluorosilicone, FPMS-123, from Gelest, Inc. (Morrisville, PA) were used in the wetting experiments. The fluorosilicone (surface tension 25.7 mN/m) was chosen due to a combination of a relatively low viscosity (300−350 cSt) and negligible vapor pressure, which allowed for a larger time window for contact angle measurements.

Carbon nanotubes and carbon films were dried overnight (100 °C) after the neutralization of the NaOH solution and were subsequently annealed in a vacuum furnace (Solar Atmosphere) with graphite heating elements under a pressure of $\sim 10^{-6}$ Torr for 2 h at 900, 1200, 1500, 1750, 1850, and 2000 °C. The lowest temperature has been chosen to be just below the threshold of 1000−1100 °C, at which bonds of functional end-groups break up,[10] leaving the nongraphitic carbon devoid of functional groups. The upper limit was set at 2000 °C because at higher annealing temperatures, incipient polygonization of CNTs occurs.[26] GL-200 glassy carbon, which was manufactured at 2000 °C,[26] does not undergo structural changes in the temperature range studied[10] and for this reason was chosen as a substrate for the CVD-carbon film deposition.

The annealed samples were characterized with a Raman spectrometer (Renishaw 1000) using an Ar ion laser (514.5 nm excitation wavelength). An XL30 (FEI) environmental scanning electron microscope (ESEM) was used to image water inside and outside CNTs. Water was condensed inside the chamber of the ESEM under pressures of up to 10 Torr and a temperature of 4−5 °C. The temperature was controlled with a Peltier cooling stage. JEOL 2010F TEM was used to image the walls of the carbon nanotubes.

Contact angle measurements were performed on drops positioned on the CVD-carbon film in air at room temperature using the sessile drop method immediately after annealing. Still images and movies were acquired using a CCD camera and were used to measure the contact angle.[4]

Conductivity measurements were performed on an individual carbon nanotube placed in position by a dielectrophoretic method[27,28] to bridge a 7 μm gap (l_{gap}) between two Au (100 nm)/NiCr (10 nm adhesion layer) electrodes evaporated on a 1 μm thick SiO_2 layer on a silicon wafer. The Au/NiCr electrodes were patterned by a photolithography and wet etching process. The current (I) through the tube was measured at room temperature in air as a function of voltage (V) using a HP 4145B parameter analyzer. The electrical conductivity of the tube was estimated from the $I-V$ curve. Prior to the measurements, the hysteresis and contact resistance were removed by increasing the tube's temperature. This was accomplished with Joule heating generated by passing relatively high currents (up to above 1 mA for annealed tubes) through the tubes for a few seconds. The $I-V$ measurements were carried out after ensuring that the shape of the $I-V$ curves was repeatable without noticeable hysteresis.

Results and Discussion

Material Characterization. TEM micrographs of the walls of as-produced nanotubes show a disordered structure typical of low-temperature pyrolitic carbon deposited by CVD (Figure 1a). Little difference is seen in the wall structure of the CNT

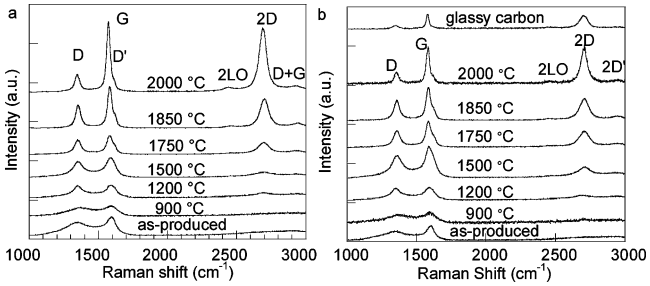

Figure 2. Raman spectra for (a) carbon nanotubes and (b) carbon films on glassy carbon. A more intense and narrow G-band and a decreasing D-band suggest the formation of a more ordered graphitic structure with an increasing annealing temperature. The appearance of a strong second-order 2-D peak is also indicative of graphitization.

annealed up to 1200 °C (Figure 1b), while partial ordering is visible at 1500 °C (Figure 1c). Increasing order of the nanotube walls is seen at 1750 and 1850 °C (Figure 1d,e). Continuous and almost perfectly ordered graphitic walls were observed after annealing at 2000 °C (Figure 1f), with the measured interplanar spacing close to that of planar graphite (0.335 nm).[10]

Further analysis of the graphitization process was conducted using Raman spectroscopy. The change of Raman spectra for carbon nanotubes (Figure 2a) and films (Figure 2b) as a function of annealing temperature has been investigated. The relative intensity of the peak at about 1350 cm^{-1}, which is attributed to the disorder-induced band of graphitic carbon (D-band), as compared to the G-band around 1580 cm^{-1}, which is assigned to in-plane vibrations of graphite, decreases with increasing annealing temperature. The G-band narrows in width due to the ordering of the turbostratic carbon, leading to a more and more graphitic structure.[29] The peak at 2450 cm^{-1} has been attributed to overtone mode longitudinal optical (LO) phonons (2LO).[30] The second-order peak at 2700 cm^{-1} is assigned to 2D vibration, and its increase is related to the ordering of the graphitic structure.[29] Finally, a less distinct peak around 2930 cm^{-1} appearing with an increasing annealing temperature is attributed to D + G vibrations. As a result of the graphitization process, the position of the G-band for tubes annealed at 2000 °C approaches the theoretical value for planar graphite. Similarly, the ratio of the intensities of the D- and G-bands, I(D)/I(G), changes from an initial value of 0.78 for as-produced nanotubes to a maximum of 0.89 for CNT annealed at 1200 °C, and to a minimum of 0.27 for tubes annealed at 2000 °C, with a change in pace between 1500 and 1750 °C annealing temperatures (Figure 3, △ for CNT and ◇ for CVD-carbon films). This ratio can be used to determine the size of the graphite crystals.

The in-plane size of graphite crystallites, L_a,[29] was obtained from statistical image analysis of the TEM micrographs of the CNT walls (Figure 1) and from Raman spectroscopy using the Tuinstra−Koenig equation:[31]

$$\frac{I(D)}{I(G)} = \frac{C(\lambda)}{L_a}$$

where C (514.5 nm) is ∼4.4 nm.[32,33]

The values measured by both techniques follow a similar behavior, although the large scatter in the Raman values (Figure 3, ○) is attributed to the influence of surface terminations and defects,[29] which have less influence on the TEM measurements (Figure 3, ■). As expected, in both cases, L_a increased exponentially with the annealing temperature in the range from 1200 to 2000 °C. The temperature dependence of grain growth

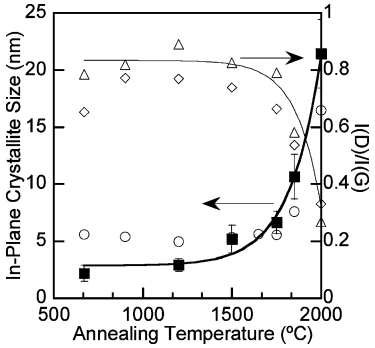

Figure 3. In-plane crystallite size, L_a, and I(D)/I(G) ratio as a function of the annealing temperature: (○) L_a values obtained from Raman spectra of CNT using the Tuinstra−Koenig equation and (■) L_a values obtained from statistical analysis of TEM micrographs of CNT. I(D)/I(G) ratio as a function of annealing temperature for CNT (△) and CVD-carbon film (◇).

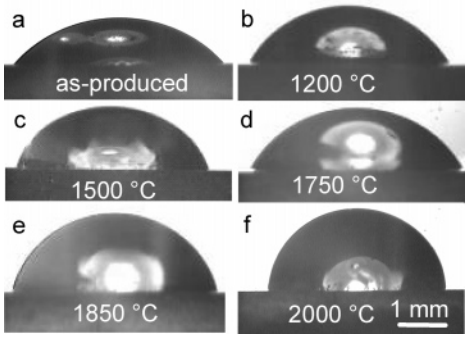

Figure 4. Optical images of water droplets on CVD-carbon films treated with NaOH. The contact angle increases with the annealing temperature: (a) 44°, (b) 54°, (c) 57°, (d) 69°, (e) 71°, and (f) 77°.

is expected to obey an Arrhenius relationship. Fitting the data as an Arrhenius equation plus an initial term accounting for the as-produced sample (670 °C), $L_a = A_0 + A \exp(-T_c/T)$, leads to a good fit with a correlation factor of 0.995 (Figure 3, fit of ■). However, plotting the data as an Arrhenius plot, ln(L_a) versus $1/T$, has shown a change in the graphitization mechanism between 1500 and 1750 °C. On the basis of FTIR data, we know that there is a loss of graphite edge plane termination at temperatures below 1500 °C. Elimination of the edge termination, which is believed to be hydrogen inside the carbon layer, allows a merger of graphite basic structure units and an increase in the in-plane crystallite size. Above a certain temperature, when no hydrogen is left in the carbon structure, grain boundary diffusion leads to further growth of the basic structure units of graphite, increasing L_a and leading to the formation of ordered graphitic walls in carbon nanotubes. Bulk diffusion of carbon can probably be neglected because the self-diffusion coefficient of carbon in graphite is very low at temperatures up to 2000 °C.[10]

Contact Angle Measurements. Figure 4 depicts images of water droplets on CVD-carbon films treated with NaOH. Similar images were used to calculate contact angle values. The results of these measurements are summarized in Figure 5. The contact angle for water increased nearly linearly from 44 ± 2° for as-produced and NaOH treated samples (synthesis temperature 670 °C) up to a value of 77 ± 2° for samples annealed at 2000 °C (Figure 5, ■). This value is close to that of hydrogen terminated CVD-carbon (76°).[4] The data were fitted with a straight line, $\theta = 31.00 + 0.02T$ (correlation factor 0.98), where θ is the contact angle and T the temperature. A contact angle in the range of 82−86° was calculated for T = 2600−2800 °C, where

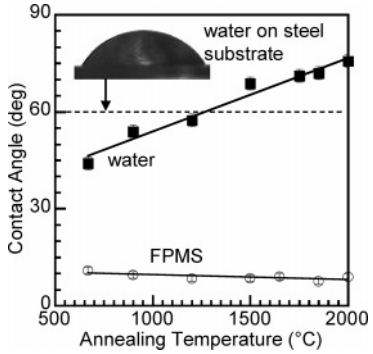

Figure 5. Contact angle on CVD-carbon film deposited on glassy carbon: contact angle for (■) water and (○) FPMS as a function of annealing temperature.

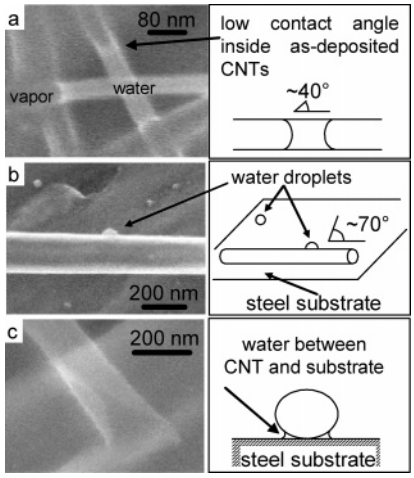

Figure 6. ESEM micrographs of wetting experiments: (a) preferential condensation of water inside an as-deposited CNT at 4 °C. (b) Water droplets condensing on the steel substrate (contact angle 55°) rather than inside an annealed (2 h at 1750 °C) tube. A water droplet with a high contact angle is observed on the external surface of CNT. (c) Water condensing between annealed CNT and steel substrate.

complete graphitization of CVD-carbon occurs.[16] This result is in agreement with the value of about 80 ± 4° calculated from AFM force measurements on carbon nanotubes dipped in water[34] as well as with contact angle measurements of water on graphite.[7,8,35]

A plot of contact angle data with L_a showed an initial steep increase and a subsequent steady value, with the slope change occurring between 1500 and 1750 °C—at about the same temperature at which the I(D)/I(G) ratio underwent a change of slope when plotted against the annealing temperature (Figure 3, △). Hence, the initial steep change in contact angle was attributed mainly to surface chemistry changes, with the progressive elimination of C−H bonds starting around 1100−1200 °C.[10] Above 1500 °C, the water's contact angle increase was attributed mainly to the progressive substitution of graphite edge sites with planar graphite planes (L_a increase in Figure 3, ■). The low contact angle for water on the as-produced surface (after NaOH treatment) is in good agreement with ESEM observations of low contact angle menisci inside both CVD-carbon nanotubes with diameters of 60 nm (Figure 6a) and 200 nm.[1] Water condensation was always first observed on the outer surface of or inside as-produced CVD tubes, never on the steel substrate, because the contact angle of water on CVD-carbon is lower than on the steel sample holder (61 ± 2°). Condensation occurs preferentially inside the tubes due to a high curvature of the inner interface of small diameter tubes (Laplace pressure).

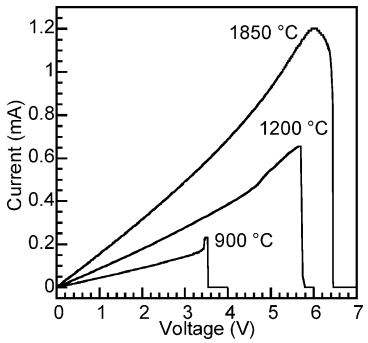

Figure 7. Current−voltage measurement of a single CNT after annealing at 900, 1200, and 1850 °C.

Although condensation may have eventually occurred also in the wedge between the tube and the steel sample holder, this could not be observed because of the presence of liquid inside the tube. When similar experiments were repeated with annealed CNTs (2 h at 1750 °C), as the pressure increased, water droplets condensed first on the steel substrate (Figure 6b) and then in the wedge between the tube and the steel holder (Figure 6c) rather than inside the annealed CNT because of its lower contact angle as compared to that of the annealed CNT (71°).

Control over the wettability of the nanotube walls can be used to modify the flow rate of liquids inside the tubes to adjust it to biological channels[5] or to supply polar or nonpolar drug solutions. We have previously demonstrated controlled condensation of water on a selected tube end by making it more hydrophilic than the other end.[36] Carbon tubes with controlled wetting properties can be used as test tubes for in situ physical and chemical experiments on a variety of liquids.

In the case of fluorosilicone, contact angles showed a weak decrease ($\theta = 11.187-0.001T$, correlation factor 0.741) from 10.9 ± 0.5° for as-produced carbon to 8.9 ± 0.5° for carbon annealed at 2000 °C. These values are in agreement with those we reported for other nonpolar liquids on CVD-carbon.[4] For the nonpolar liquid, good wetting was observed over the entire annealing temperature range (Figure 5, ○). This shows that use of nonpolar solvents is preferred when a good dispersion of nanotubes must be achieved, whether for microscopy sample preparation or for composite manufacturing.

Conductivity Measurements. Next, we studied the electrical transport characteristics of the carbon nanotubes after undergoing annealing at various temperatures. Figure 7 depicts the current I (mA) as a function of the potential difference V (V) of carbon nanotubes annealed at 900, 1200, and 1850 °C. The $I-V$ curves exhibit nearly linear behavior over a broad range of voltages. Nonlinearity in the $I-V$ curves becomes noticeable at higher voltages near the tube's breakdown, where the current drops abruptly to zero. The tube breakdown occurs, respectively, at the peak conductance ($\sigma_{peak} = I_{break}/V_{break}$) values of 7×10^{-5}, 1×10^{-4}, and 2×10^{-4} S for the 900, 1200, and 1850 °C tubes, respectively. We suspect that the tube's breakdown was caused by ohmic heating and the tube's oxidization.[37,38] Because of the breakdown, the power increased from about 0.7 to 3.5 to 7.8 mW as the annealing temperature increased from 900 to 1200 to 1850 °C. Since the heat transfer from the carbon tubes is dominated by heat dissipation to the ambient, the data indicate that the tubes annealed at higher temperatures were able to withstand higher temperatures during current transmission without oxidizing. It is known that oxidation of ordered carbon nanostructures occurs at higher temperatures as compared to disordered carbon.[39]

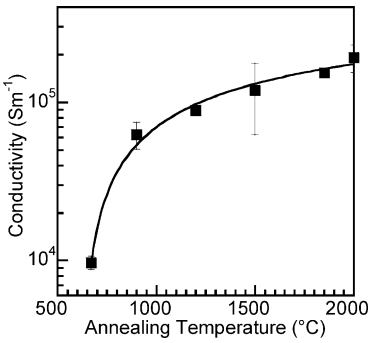

Figure 8. Conductivity measurement of single CNT across two gold electrodes as a function of the annealing temperature.

Figure 8 depicts the conductivity (S) of the carbon nanotubes as a function of the annealing temperature. The conductivity was estimated using the formula $\sigma_{peak} l_{gap}/A_{tube}$, where A_{tube} is the cross-sectional area of a carbon tube with a wall thickness of 20 nm and an outer diameter of 300 nm.

The conductivity of the carbon nanotubes increased from about 1×10^4 S/m in the as-produced tubes (670 °C) to 2×10^5 S/m after annealing at 2000 °C. Witness the rapid increase of the conductivity with the annealing temperature for relatively low annealing temperatures (<900 °C) and the gradual, monotonic increase between 900 and 2000 °C (Figure 8). A similar behavior, observed previously upon annealing of amorphous carbons, was attributed to a strong reduction of the band gap.[40] This result is in agreement with our observations of a pronounced reduction of the tube transparence to white light when conducting nanofluidic experiments with as-produced and annealed tubes under a light microscope.

Interestingly, the measured conductivity values of the carbon nanotubes range from the conductivity of low-temperature, hydrogen-terminated disordered graphitic carbon to the in-plane conductivity of pure graphite.[9−12] When plotted as a function of L_a, the conductivity experienced an initial steep increase, then remained level once L_a exceeded 5 nm. We believe that the initial growth in conductivity occurred due to the elimination of the edge termination of graphene sheets, which occurs at temperatures below 1200 °C. At higher temperatures, most of the hydrogen and oxygen should be gone, and the tube walls consist of pure graphite with a very low content of functional groups. A strong decrease in the intensity of C−H vibrations was also observed by FTIR after annealing (not shown in the paper).

On the basis of the possibility of tailoring the electrical conductivity through graphitization, CVD-nanotubes could fill the gap between insulating or poorly conducting inorganic nanotubes (SiO_2, BN, or TiO_2) and MWCNTs for ionic current exchange between cells and nanofluidic devices.[2]

Conclusion

Annealing can be used to control surface and bulk properties of carbon nanotubes and thin films produced by CVD. In particular, the contact angle of water increased by a factor of 2 (from 44 to 77°), and the bulk electrical conductivity of nanotubes increased by a factor of 20 after annealing at 2000 °C. Both the contact angle and the conductivity followed a similar behavior when plotted against the in-plane crystallite size of graphite, with an initial steep increase followed by a slow growth. We suspect that the fast increase in the contact angle and electrical conductivity as a function of annealing temperature below 1500 °C is primarily due to the elimination of edge-plane terminations rather than an increase of L_a. Excellent wetting and small contact angles were observed for water condensed inside as-produced 60 and 200−300 nm tubes with disordered carbon walls. Condensation of water occurred outside of CNTs after annealing at 1500 °C and above. At the same time, the annealing had little effect on wetting of carbon with nonpolar fluorosilicone.

Acknowledgment. This research was supported by NSF NIRT Grant CTS-0210579. The authors are thankful to Dr. H. Ye for assistance with the TEM studies and Dr. S. Babu and Prof. J.-C. Bradley for developing the process of making alumina membranes with 60 nm pores. The ESEM and Raman spectrometer are operated by the centralized Materials Characterization Facility of the A. J. Drexel Nanotechnology Institute. TEM work was carried out in the LRSM, University of Pennsylvania. The vacuum furnace was donated by Solar Atmospheres, PA.

References and Notes

(1) Rossi, M. P.; Ye, H. H.; Gogotsi, Y.; Babu, S.; Ndungu, P.; Bradley, J. C. *Nano Lett.* **2004**, *4*, 989.
(2) Fan, R.; Yue, M.; Karnik, R.; Majundar, A.; Yang, P. *Phys. Rev. Lett.* **2005**, *95*, 086607.
(3) Bau, H. H.; Gogotsi, Y.; Megaridis, C. M.; Bradley, J. C. *J. Fluids Eng.* **2006**, *128*, 3.
(4) Mattia, D.; Bau, H. H.; Gogotsi, Y. *Langmuir* **2006**, *22*, 1789.
(5) Majumder, M.; Chopra, N.; Andrews, R.; Hinds, B. J. *Nat. Mater.* **2005**, *438*, 44.
(6) Kim, B. M.; Sinha, S.; Bau, H. H. *Nano Lett.* **2004**, *4*, 2203.
(7) Fowkes, F. M.; Harkins, W. D. *J. Am. Chem. Soc.* **1940**, *62*, 3377.
(8) Morcos, I. *J. Colloid Interface Sci.* **1970**, *34*, 469.
(9) Wang, Y.; Santiago-Aviles, J. J.; Furlan, R.; Ramos, I. *IEEE Trans. Nanotechnol.* **2003**, *2*, 39.
(10) Pierson, H. O. *Handbook of Carbon, Graphite, Diamond, and Fullerenes*; Noyes Publications: Park Ridge, NJ, 1993.
(11) Jang, W. Y.; Kulkarni, N. N.; Shih, C. K.; Yao, Z. *Appl. Phys. Lett.* **2004**, *84*, 1177.
(12) Zhang, L.; Austin, D.; Merkulov, V. I.; Meleshko, A. V.; Klein, K. L.; Guillorn, M. A.; Lowndes, D. H.; Simpson, M. L. *Appl. Phys. Lett.* **2004**, *84*, 3972.
(13) Andrews, R.; Jacques, D.; Qian, D.; Dickey, E. C. *Carbon* **2001**, *39*, 1681.
(14) Kouklin, N. A.; Kim, W. E.; Lazareck, A. D.; Xu, J. M. *Appl. Phys. Lett.* **2005**, *87*, 173901.
(15) Kyotani, T.; Tsai, L.; Tomita, A. *Chem. Mater.* **1996**, *8*, 2109.
(16) Delpeux-Ouldriane, S.; Szostak, K.; Frackowiak, E.; Beguin, F. *Carbon* **2006**, *44*, 814.
(17) Che, G.; Lakshmi, B. B.; Martin, C. R.; Fisher, E. R. *Chem. Mater.* **1998**, *10*, 260.
(18) Miller, S. A.; Young, V. Y.; Martin, C. R. *J. Am. Chem. Soc.* **2001**, *123*, 12335.
(19) Kyotani, T.; Tsai, L.; Tomita, A. *Chem. Mater.* **1995**, *7*, 1427.
(20) Masuda, H.; Fukuda, K. *Science* **1995**, *268*, 1466.
(21) O'Sullivan, J. P.; Wood, G. C. *Proc. R. Soc. London* **1970**, *317*, 511.
(22) Thomson, G. E.; Xu, Y.; Skeldon, P.; Shimizu, K.; Han, S. H.; Wood, G. C. *Philos. Mag. B* **1987**, *55*, 651.
(23) Furneaux, R. C.; Rigby, W. R.; Davidson, A. P. *Nature* **1989**, *337*, 147.
(24) Sadasivan, V.; Richter, C. P.; Menon, L.; Williams, P. F. *AIChE J.* **2005**, *51*, 649.
(25) Xu, T. T.; Piner, R. D.; Ruoff, R. S. *Langmuir* **2003**, *19*, 1443.
(26) Gogotsi, Y.; Libera, J.; Kalashnikov, N.; Yoshimura, M. *Science* **2000**, *290*, 317.
(27) Riegelman, M.; Liu, H.; Evoy, S.; Bau, H. H. In *Nanoengineered Nanofibrous Materials*; Guceri, S., Gogotsi, Y. G., Kuznetsov, V., Eds.; NATO Science Series II, Mathematics, Physics and Chemistry; Kluwer: Dordrecht, The Netherlands, **2004**, *169*, 409.
(28) Riegelman, M.; Liu, H.; Bau, H. H. *J. Fluids Eng.* **2006**, *128*, 6.
(29) Ferrari, A. C.; Robertson, J. *Phys. Rev. B* **2000**, *61*, 14095.
(30) Shimada, T.; Sugai, T.; Fantini, C.; Souza, M.; Cancado, L. G.; Jorio, A.; Pimenta, M. A.; Saito, R.; Gruneis, A.; Dresselhaus, G.; Dresselhaus, M. S.; Ohno, Y.; Mizutani, T.; Shinohara, H. *Carbon* **2005**, *43*, 1049.
(31) Tuinstra, F.; Koenig, J. L. *J. Chem. Phys.* **1970**, *53*, 1126.
(32) Knight, D. S.; White, W. B. *J. Mater. Res.* **1989**, *4*, 385.
(33) Matthews, M. J.; Pimenta, M. A.; Dresselhaus, G.; Dresselhaus, M. S.; Endo, M. *Phys. Rev. B* **1999**, *59*, R6588.

(34) Barber, A. H.; Cohen, S. R.; Wagner, H. D. *Phys. Rev. Lett.* **2004**, *92*, 186103.
(35) Ogarev, V. A. *Colloid J. USSR* **1978**, *40*, 153.
(36) Babu, S.; Ndungu, P.; Bradley, J. C.; Rossi, M. P.; Gogotsi, Y. *Microfluidics Nanofluidics* **2005**, *1*, 284.
(37) Collins, P. G.; Hersam, M.; Arnold, M.; Martel, R.; Avouris, P. *Phys. Rev. Lett.* **2001**, *86*, 3128.
(38) Lee, S. B.; Teo, K. B. K.; Chhowalla, M.; Hasko, D. G.; Amaratunga, G. A. J.; Milne, W. I.; Ahmed, H. *Microelectron. Eng.* **2002**, *61*−*62*, 475.
(39) Osswald, S.; Flahaut, E.; Ye, H.; Gogotsi, Y. *Chem. Phys. Lett.* **2005**, *402*, 422.
(40) Carmona, F.; Delhaes, P.; Keryer, G.; Manceau, J. P. *Solid State Commun.* **1974**, *14*, 1183.